International Journal of Technology 13(3) 533-543 (2022)
Received August 2021 / Revised September 2021 / Accepted January 2022

International Journal of Technology
http://ijtech.eng.ui.ac.id

Towards Understanding of Pore Properties of polystyrene-b-polybutadiene-b-polystyrene (SEBS) Foam Effect on Thermal Conductivity Using Numerical Analysis

Muhammad Zulkarnain[1*], Rahida Wati Sharudin[2], Masahiro Ohshima[3]

[1]*Fakulti Teknologi Kejuruteraan Mekanikal dan Pembuatan, Universiti Teknikal Malaysia Melaka (UTeM), 75450 Ayer Keroh, Malacca, Malaysia*
[2]*School of Chemical Engineering, College of Engineering, Universiti Teknologi MARA (UiTM), 40450 Shah Alam, Malaysia*
[3]*Department of Chemical Engineering, Kyoto University, Kyoto 615-8510, Japan*

Abstract. Thermoplastic elastomer Polystyrene-b-polybutadiene-b-polystyrene (SEBS) foams are prepared by using carbon dioxide (CO2) as a blowing agent via a pressure quench method. During the foaming process, various pore shapes are developed inside the foam, which is influenced by several parameters such as rigidity, solubility, and diffusivity of CO2. A previous study revealed the theory of how SEBS foams may shrink due to low rigidity and high CO2 diffusivity, but empirical verification on how the final cell properties like cell shape, cell size, cell distribution, and percentage of porosity may affect the thermal conductivity of SEBS foam is challenging to represent experimentally. This is due to difficulty in preparing foam samples at different cell shapes for the same polymer, different percentages of porosity, and cell distribution while keeping the same cell size of the SEBS foam. This paper discussed how numerical analysis is employed to investigate various properties of pores such as cell shape, cell size, cell distribution, and percentage of porosity on the thermal conductivity. The simulation results are corroborated with experimental value where the reduction of thermal conductivity is observed with a higher percentage of porosity which is shown by all cell shapes foam such as spherical, ellipse, and irregular.

Keywords: Numerical; Polystyrene-b-polybutadiene-b-polystyrene (SEBS); Pore; RVE.

1. Introduction

Polymer foams are a class of lightweight materials that possess unique properties and amazing versatility (Monie et al., 2021). They are found virtually everywhere, either in liquid or solidified form. They are widely used for packaging applications by their porous structure and superior properties of the low density of foams. The advancement of foaming technology is still in progress because the demand for foam products is widely expanded nowadays. The cell properties and cellular structure are highly dependent on their application. The essential concerns for these Polymer foams are their final foam structures and cell properties to achieve a high functionality-to-weight ratio for any polymer foam materials. To improve the thermal insulating properties of foam materials the average cell size of foam must be reduced to approach the mean free path of gas molecules in the air, as the thermal properties of air are comparable to the thermal properties of foam in a vacum

*Corresponding author's email: m.zulkarnain@utem.edu.my, Tel.: +606-2701184, Fax: +606-2701064
doi: 10.14716/ijtech.v13i3.5097

(Dai et al., 2021). In biomedical applications, the requirement to be met as a bioscaffold is higher porosity, adequate pore size, structural integrity, and shape stability to the tissue defect to enable tissue regeneration during implantation (Roedel et al., 2018).

The relationship between foam properties and its overall performance needs to be well understood by properly designing the polymer foam structure. Such an optimized cell structure design will provide superior properties by resulting in high strength, good heat transferability, and good performance to the targeted application foam. Therefore, it is vital to design the foam properties prior to preparing the foam material for any specific applications. Many studies are reported on different control strategies for controlling cell properties like selecting optimum foaming conditions (Mantaranon & Chirachanchai, 2016), utilizing nucleating agent (Chauvet et al., 2016), controlling the polymer rigidity (rheological properties) (Lee et al., 2016; Rainglet et al., 2021), performing a different method of foaming (Solbakken et al., 2021; Muayad et al., 2020), utilizing different blowing agent (Coste et al., 2020), selecting an appropriate pair of polymers in case of polymer blend foam is desired and many more methods. Zakyan et al. (2014), for example, controlled foam morphology of Polystyrene (PS) via surface chemistry, size, and concentration of nano-silica particles. They found that the size of nano-silica particles as well as silica loading affected the pore size and cell density. There are are also studies reported on enhancing the pore properties of polymer foams by modifying the surface of silica nanoparticles (Rende et al., 2013) and controlling cell size and number of cells by using surfactant (Eaves, 2004). It is found that surfactants can produce a higher miscibility rate of the polymer blends by reducing surface tension. On the other hand, cell openers can be utilized to improve the dimensional stability of the foam.

Generally, polymer foam can be prepared either by thermoplastic or a thermoset polymer. A thermoplastic-based foam usually has characteristics of stable sphere dimension if foaming conditions like temperature are adequately controlled at a temperature near either Tg or Tm of the polymer. On the other hand, stable dimension thermoset-based foam only can be successfully prepared when the appropriate degree of curing or cross-linking for foaming and cell stabilization are satisfied. In case of thermoplastic elastomer (TPE) that has combinational properties of thermoplastic polymer and rubber is more likely complicated to be foamed as it may shrink and less uniform if the cross-linked chains are reduced, low solubility, as well as high blowing agent diffusivity and low rigidity, is possesses by the TPE (Sharudin & Ohshima, 2012).

The overall performance of polymer foam is highly dependent on and defined by its cell properties are reported elsewhere (Sundarram & Li, 2013; Jana et al., 2016; Shang et al., 2017). A typical conductivity test is commonly utilized to investigate the thermal conductivity performance of the foam. However, FEA enables designing and quantifying heat transfer profile in the region of the foam as well as enables to interpret the thermal conductivity- cell properties relationships. However, polymer foams as an insulator are important to design their quantifying heat transfer profile that relates to cell properties relationships. Although some analytical and FEA examples of the foam proposed the design, few analytical which introduce various shapes and randomly distributed on polymer foam have been rarely reported.

Realizing the lack of information regarding foam properties focused on its cell shape, this study focuses on designing cell properties for making a good thermal insulator by employing Finite Element Analysis (FEA). FEA has been established and successfully used in various fields. Previous researchers successfully analyzed complex cell structures to apply in several applications such as dentistry, orthopedics, polymer scaffold architecture, and the engineering field (Moratal, 2010). To clarify this thermal behavior and its

conductivity profile, we used FEA to calculate the thermal conductivity. We investigated the temperature profile of two grades of SEBS foams by PS and polypropylene (PP) blend to observe the cell sizes, distribution, shape, and it's porosity performance. Thus, this study explains the application of FEA in designing thermal insulators of elastomer-based foam at various cell shapes, cell sizes, and percentages of foam porosity. The FEA results are then validated with experimental data.

2. Methods

2.1. Materials

SEBS copolymer grade H1062 was supplied by Asahi Kasei Elastomer. H1062 is composed of 18 wt% styrene blocks and 82 wt% ethylene-butylene blocks, and its average molecular weight is 70,000 g mol-1. SEBS grade H1043 consists of 33 wt% of styrene segments while the remaining is butadiene at 67 wt%. Homo-Polypropylene (PP, Mw= 410,000) was supplied by Mitsubishi Chemical, and Polystyrene (PS, Mw= 192,000) was obtained from Aldrich Chemical Co. All polymers were used as received. The SEBS copolymer grade H1062 cellular structures are shown in Figure 1.

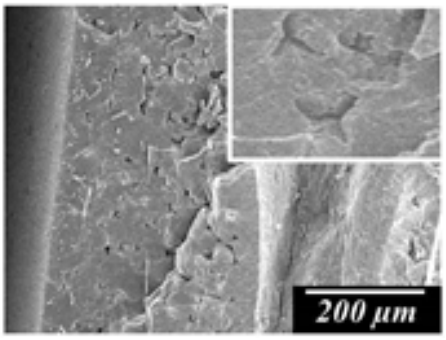

Figure 1 Cell morphologies of SEBS H1062 foam

The procedures detail can be illustrated as shown in Figure 2, where the final foam is produced at three stages conditions. In the first stage, the SEBS H1062 with styrene segments of 18 wt.% were foaming at elevated foaming temperatures after six hours of CO_2 dissolution at 10 MPa. In the second stage, the foam runs into desorption polymer under supersaturated condition, while in the last phase, the foam becomes saturated condition and foam already prepared. It was observed that the cell structures of SEBS H1043 foams appeared as a sphere- shaped designs at all ranges of foaming temperature, while SEBS H1062 foams appeared as star-shaped structures.

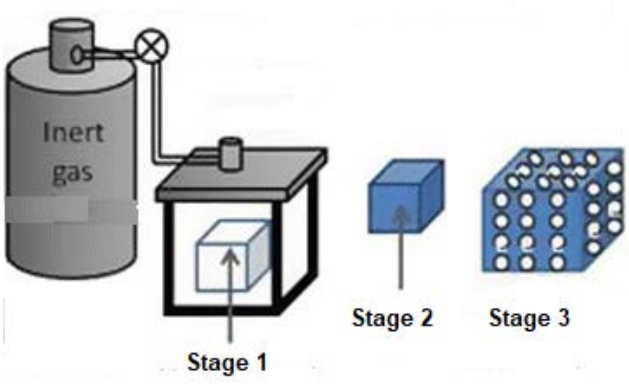

Figure 2 Polymer foam procedure

2.2. Experimental Measurements

The thermal conductivity of foam samples was measured by using the SOLTEQ® Thermal Conductivity of Solids, Liquids, and Gases Unit (Model: HE116). Samples were first inserted into the unit and clamped by the heating plate. The temperature controller for hot plates was set at 50°C. The reading for hot plate and cold plate temperatures, as well as heat flux, was recorded when the temperature controller was stable. This study considered the single plate method where the heat flux and thermal conductivity of foam samples are calculated by the following equations:

Heat transfer rate,

$$q = -kA\frac{\partial T}{\partial x}\ ,\ (\frac{W}{m^2.K}) \quad (1)$$

Thermal conductivity,

$$k = -\frac{q.x}{A(T_2-T_1)}\ ,\quad (\frac{W}{m.K}) \quad (2)$$

Where k is thermal conductivity. A is a cross-sectional area of the sample, T_2 is hot plate temperature, and T_1 is cold plate temperature.

2.3. Numerical Analysis

The mesh number is above 300,000 to obtain accurate results of thermal conductivity. The grid dependence study of the domain was run for different mesh numbers to check the grid dependency of the model size case. A dependency study is conducted in simulations to obtain accurate and cost-effective results.

2.3.1. Cell Shape Generating

This investigation proposes several cell structures such as irregular shapes, ellipses, and spherical pores by using the random distribution technique for thermal analysis. Types of microstructures are considered in non-overlapping conditions. Figure 4 illustrates the different shape probabilities of pores in the microstructure of porous materials. Three different shapes of pores are studied in the thermal analysis with named type A (irregular), B (ellipse), and C (sphere). For rough shape, the probability shape is constructed by Voronoi formulated in commercial MATLAB as shown in Figure 3 (a) as named by type A. A specific space with eight cubical points is constructed to generate the irregular cell. In this space size, the point is launched at a random location. Next, the Voronoi codes in commercial MATLAB will give the face closed all random points presented as the random shape. The pore shape is exported to a CAD system for compatibility using Finite Element Analysis code. At the same time, type B and C are denoted to ellipse and spherical shapes, respectively. Type B and C are primitive geometry that CAD systems can generate in the ANSYS workbench facility.

2.3.2. Convergence Study

The thermal conductivity values against the various model sizes are plotted for the convergence study. Some fixed value of conductivity or small fluctuated conductivity value of a certain model size is carried out. The thermal conductivity value is then validated with experimental results. In this convergence study, the model size is determined to represent the proper RVE size model based on Table 1, and the cell size is fixed at 2 μm.

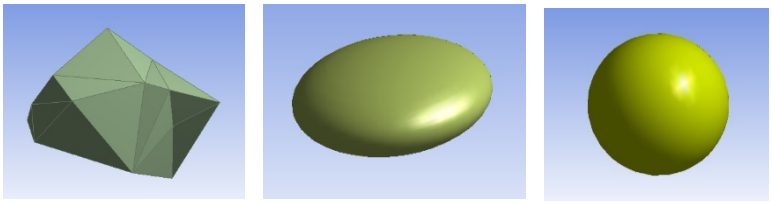

(a) (b) (c)

Figure 4 Probability of three pore shapes; (a) Type A is irregular, (b) Type B is ellipse and (c) Type C is spherical

Table 1 Thermal conductivity of multiple shape pores against size.

Size (μm)	Type A (W/mK)	Type B (W/mK)	Type C (W/mK)
0.2	0.17064	0.16956	0.15707
2	0.17062	0.16959	0.15741
30	0.17072	0.16958	0.15697

2.3.3. Volume Fraction Study

The thermal conductivity study is presented by plotting the effect of the volume fraction of pores material on thermal conductivity. The volume fraction is varied in the range of 5%, 10%, 15%, and 24% by comparing the matrix volume. In contrast, the model size is fixed at $\delta = 5$.

The geometry construction is designed with a cubical block that is embedded in cell structure. The critical part of geometry construction focuses on the cell structure and their portioning. This is due to the cell structure will determine the final output of thermal properties of the model. The particles dispersion is designed at the first step in creating the geometry to avoid any mistakes and then followed by a cubical block as shown by previous method (Zulkarnain M. et al. 2007). Cell structure number embedded in the cubical block was determined by volume fraction. The formula for volume fraction conducted in this study is using spherical volume approach to calculate the cell volume as presented by the equation below (Zulkarnain M. et al. 2007):

$$Vol.\% = \frac{(4/3)\pi r^2 (n)}{(w \cdot h \cdot l)} \tag{3}$$

The notation n denotes the amount of cell filling, while w, h, and l are width, height, and length of modeling size, respectively. In this case, the numbers of cells generated at 24% of the cell volume fraction. Both phases, matrix, and pores, present a linear thermal conducting, while the model size was adopted from the previous method (Zulkarnain M. et al. 2007). The considered thermal conductivity for the matrix phase is SEBS and the pores are considered as SEBS cells containing air as shown Figure 5.

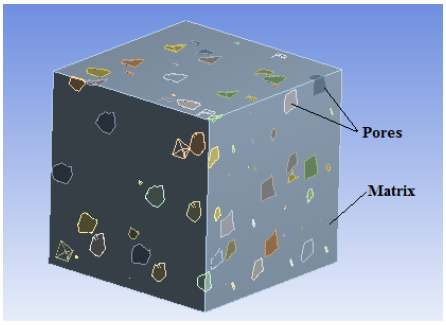

Figure 5 Porous microstructures of morphological parameters of the un-void condition

3. Results and Discussion

3. 1. Experimental Results

The cell shape of SEBS foam at foaming temperature 60°C has presented the conductivity value was in the range 0.1504-0.1652 W/m.K with density given at 0.75 g/cm^3, while the specific cell shape was described in a sphere with a diameter of 15 μm. Figure 6 shows the cellular structure of SEBS blend foams prepared at 10 MPa with various cell shapes. Furthermore, as can be seen in the figure, the cells' SEBS blend foam was various, and the distance between cells was closer, which is dictated the ease of heat transfer. According to Marshall (2012), to increase the thermal stability, the thermal transfer should be improved the cell numbers to bridge the thermal network.

The effect of cell size on the thermal conductivity of elastomer foams was further investigated by comparing two different cell sizes of 20 μm for SEBSH1062/PS blend foams. It was taught that the thermal conductivity of foam samples decreased with the increase in cell size. The thermal conductivities of SEBS foam in various shapes presented at 0.1652 W/m.K (Star shape), 0.1504 W/m.K (sphere shape), and 0.1259 W/m.K (irregular shape).

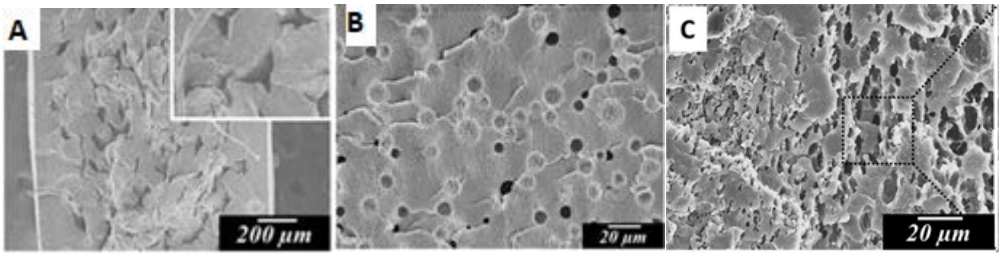

Figure 6 Cell morphologies of SEBS with certain shapes; (A) star, (B) sphere and (C) irregular.

3.2. Results of Finite Element Analysis of RVE Aize

The Representative Volume Element (RVE) sizes models for thermal homogenization of porous materials are first constructed. Based on thermal conductivity predicted at various pore shapes based on various size (δ) RVE model, it shows that the thermal conductivity results decrease when the size of the RVE model increases. For each numerical results, it is found that the RVE size model for all cases is fluctuated or leads to a constant direction when the RVE size is at $\delta = 5$. Therefore, it is chosen as a representative size to describe the thermal behaviour of random porous microstructures for any volume size of porous materials such suggested by previous researchers (Moumen et al., 2015).

3.3. Cell Size Effect

To obtain good predictions of the pore's material in the thermal application, pore size is also discussed in this part. The modeling is simulated at 24 vol.% of volume fractions with $\delta = 5$ for model size. The results show that the pore size presents an insignificant effect on the thermal conductivity, as listed in Table 1.

3.4. Volume Fraction Effects

The effect of volume fractions on the effective thermal conductivity of porous microstructures for various pore types is given in Figure 7. The estimated thermal conductivity decreases by increasing the pore volume fractions. Type C pore (sphere shape) shows better estimating due to higher thermal resistance. By comparing analytical results and numerical values, good estimating is given by HS-Bound for lower thermal conductivity. In addition, the numerical results are systematically analytical, which is close to homogenization approaches in the experimental method.

Type C shows higher thermal resistance with a similar microstructure pattern than other types. The estimated thermal conductivity of Type C was very close to the analytical

method proposed by Maxwell-Eucken. Considering a random microstructure (porous or composites) made of two phases, the inclusion phase (P1) with volume fraction p and matrix one (M1) with volume fraction 1 – p, it is considered they are having a real thermal conductivity of λ_1 and λ_2, respectively. The various analytical models and bounds used for thermal analysis are detailed in (Buryachenko, 2007) and are given by the following equations:

Series model

$$\lambda = \frac{\lambda_1 \quad \lambda_2}{(1-p)\lambda_1 + p\lambda_2} \tag{4}$$

Parallel model

$$\lambda = p\lambda_1 + (1-p)\lambda_2 \tag{5}$$

The Maxwell-Eucken models: Eqs. (6) and (7) are named the Maxwell-Eucken models, as Eucken has first applied the Maxwell model to a thermal problem. It is noted that the Maxwell-Eucken models require the distinction between the components, one being the dispersed phase and the other being the continuous phase (matrix). Maxwell-Eucken model 1: component 2 as the continuous phase.

$$\lambda^{eff} = \lambda_2 \frac{2\lambda_2 + \lambda_1 - 2(\lambda_2 - \lambda_1)p}{2\lambda_2 + \lambda_1 + (\lambda_2 - \lambda_1)p} \tag{6}$$

Maxwell-Eucken model 2: component 1 as the continuous phase.

$$\lambda^{eff} = \lambda_1 \frac{2\lambda_1 + \lambda_2 - 2(\lambda_1 - \lambda_2)(1-p)}{2\lambda_1 + \lambda_2 + (\lambda_1 - \lambda_2)(1-p)} \tag{7}$$

The Hashin-Shtrikman bounds model was also used to compare the predicted thermal conductivity value obtained from the FEA model (Buryachenko, 2007). The equations used are as follows:

Hashin–Shtrikman bounds:

$$\lambda^{HS+} = \lambda_2 + \frac{p}{1/(\lambda_1 - \lambda_2) + (1-p)/3\lambda_2} \tag{8}$$

$$\lambda^{HS-} = \lambda_1 + \frac{1-p}{1/(\lambda_2 - \lambda_1) + p/3\lambda_1} \tag{9}$$

In this analysis, the prediction of thermal conductivity is limited to steady-state conduction heat transfer through the internal porosity region. According to Carson et al. (2005), porous materials can be classified into internal and external porosity materials. The former is classified as the material having continuous isolated or interconnected solid matrixes that contain pores like sponge, foam, and honeycomb, while the latter refers to the material that contains granules or particulate.

At low volume percent of the pore, the thermal conductivity values for all pore types are almost similar to the conductivity values analyzed by Maxwell, Hashin and parallel models as depicted in Figure 7. When the volume percent increases up to 10 vol.%, the conductivity values are lied in between the Hashin model as the upper bound and the Maxwell model as lower bound. Moreover, above 10 vol.% up to 20 vol.% the predicted value by FEA for type C was near to Maxwell model while type A and B were approaching to Parallel and Hashin models. This implies that for irregular and ellipse shapes with more than 10 vol.% of porosity, conductivity values were not corroborated well with the Maxwell model. It is speculated that the Maxwell model assumption of the inclusion of dispersed

phase are not contacted with neighbouring inclusions is obeyed (Li et al., 2017). Hence, above 10 vol.% the probability of pores to be reached each other is ignored. Whereas for these two shapes, the predictions of thermal conductivity by FEA and Hashin are almost identical.

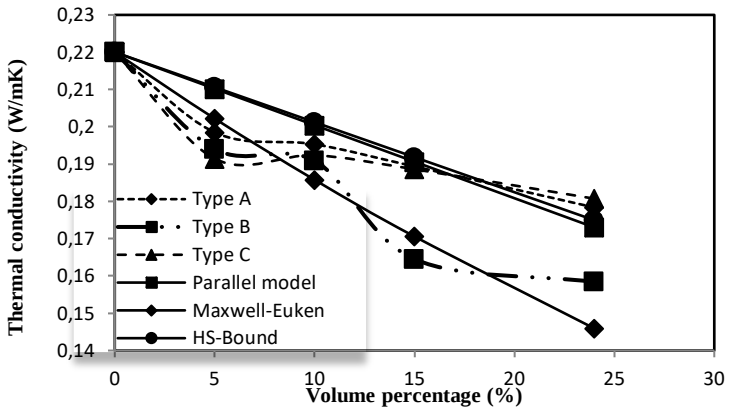

Figure 7 Thermal conductivity against volume fraction

The effect of porosity and the distribution of pores were presented in the form of a heat flux profile. The results state that heat flux intensity is reduced with the order of sphere, ellipse, and irregular pore shape. As expected, the conductivity value for the sphere pore is the lowest, which indicates the stable dimension cell would be beneficial for resisting the heat flow. It is noted that, in the case of non-overlapping spherical pores, the numerical computations are limited to 24 vol.% of volume fractions. This phenomenon also shows that the optimal heat flux through the dispersed phase is less than the continuous phase for all pore shapes, while the intensity of heat distribution in the continuous phase in irregular shapes is higher compared to the sphere and ellipse shapes. Based on the prediction by FEA that is not well corroborated with Maxwell model for type A pore, it supported the speculation of irregular shape which can represent shrunk pore or unstable dimension pore has higher thermal conductivity due to heat conduction pathway intense at matrix as compared to in ellipse and sphere. This is because heat flow essentially avoids the dispersed phase when the thermal conductivity of the matrix phase is more excellent than the thermal conductivity of the dispersed phase, it is a similar phenomenon reported by previous results (Sharudin & Ohshima, 2012). For type B and C, in which the heat distribution is more intense at dispersed phases, heat preferentially flow through this phase when the situation is in the opposite, where the thermal conductivity of dispersed phases is greater than the matrix phase. This apparent heat distribution profile for type A is supported by the Maxwell assumption that the dispersed phase never forms a continuous pathway for heat transfer perspective and had a bias towards the continuous phase (Carson et al., 2005). As the cell shrink, it is highly possible that the foam material behaves like a solid material and heat transfer through the continuous phase. At the same time, the sphere shape represents a stable dimension pore allowing the heat to transfer through the dispersed phases due to the homogeneous foam performance.

To validate the effect of morphological factors such as the porosity, the distribution, and the shape of pores on local thermal conductivity, we prepared a microcellular foam of the SEBS and their blends to obtain a cell with a sphere and irregular structures at different cell size and porosity. The conductivity values predicted by FEA are then compared to the measurements from experimental work. The thermal conductivity test was compared for both experimental and numerical SEBS foams were shown in Figure 8. The thermal conductivities of experimental SEBS foam were compared at sphere shape by a volume

percentage of 27%. Comparing the thermal conductivity results, it is noted that about 3.97% difference to Type B showed no significant effect on experimental and numerical results. By referring to the FEA analysis of the cell size effect on thermal conductivity, the predicted value shows no significant thermal conductivity change between cells having sizes of 0.2, 2 and 20 μm.

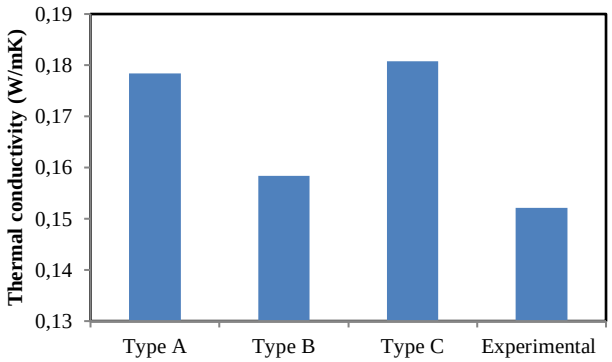

Figure 8 Thermal conductivity comparison.

4. Conclusions

The reliability of the numerical method of interpreting the thermal conductivity-cell properties relationships was supported by the analytical model of Maxwell-Eucken and further validated with the experimental results. Using the cell properties in terms of cell size, cell shape, and percentage of porosity, numerical results were able to clarify the thermal behavior of different SEBS cell shapes by their heat distribution profile. As shown in this study, the cell having an ellipse shape has lower thermal conductivity than the irregular one. However, the effect of cell size seems insignificant to the thermal conductivity value for each RVE study. The insignificant differences between the numerical and experimental results have shown it successfully demonstrated. Since preparing foam with different cell sizes while maintaining the percentage of porosity is challenging to control, the computerized approach would be affording a favorable thermal conductivity estimation alternative to enable the designing thermal insulators of elastomer-based foam at various cell properties.

Acknowledgements

On behalf of all authors, the corresponding author states that they much appreciate Universiti Teknikal Malaysia Melaka (UTeM) supporting financially by Short term grant PJP/2020/FTKMP/PP/S01765, the Research Management Centre (RMC), Universiti Teknologi MARA (UiTM) for the financial support of the project under the grant 600-IRMI 5/3/LESTARI (042/2019) and Material Process Engineering Laboratory, Kyoto University for technical support during research completion.

References

Buryachenko V., 2007. *Micromechanics of Heterogenous Materials*. 1st Edition. USA: Springer, Dayton research institute, pp. 95–136

Carson J.K., Lovatt S.J., Tanner D.J., Cleland A.C., 2005. Thermal Conductivity Bounds for Isotropic Porous Materials. *International Journal of Heat Mass Transfer*, Volume 48(11), pp. 2150–2158

Chauvet M., Fages J., Sauceau M., Bailon F., 2016. Use of Starch as Nucleating Agent for the Extrusion Foaming of Poly-(Lactic Acid). In *15th European Meeting on Supercritical Fluids, EMSF 2016*

Coste G., Negrell C., Caillol S., 2020. From Gas Release to Foam Synthesis, The Second Breath of Blowing Agents. *European Polymer Journal*, Volume 140(1). Doi: https://doi.org/10.1016/j.eurpolymj.2020.110029

Dai T.R., Chandrasekaran G., Chen J., Jackson C., Liu Y., Nian Q., Kwon B., 2021. Thermal Conductivity of Metal Coated Polymer Foam: Integrated Experimental and Modeling Study. *International Journal of Thermal Science*, Volume 169, No. 9. Doi: https://doi.org/10.1016/j.ijthermalsci.2021.107045

Eaves D., 2004. Handbook of Polymer Foams. *Rapra Technology Limited, Shrewsbury, Shropshire, United Kingdom*, pp. 72–73

Jana D.C., Sundararajan G., Chattopadhyay K., 2016. Effect of Porosity on Structure, Young's Modulus, and Thermal Conductivity of Sic Foams by Direct Foaming and Gel Casting. *Journal American Ceramic Society*, Volume 100(32), pp. 312–322

Lee W., Lee S., Izadi M., Kam S.I., 2016. Dimensionality-Dependent Foam Rhelogical Properties: How to Go from Linear to Radial Geometry for Foam Modelling and Simulation. *SPE Annual Technical Conference and Exhibition, Houston, Society of Petroleum Engineers (SPE*), Volume 21(5), pp. 1669–1687

Li X., Park W., Chen Y.P., Ruan X., 2017. Effect of Particle Size and Aggregation on Thermal Conductivity of Metal-Polymer Nanocomposites. *Journal of Heat Transfer*, Volume 139(2), pp. 022401-1–022401-5

Mantaranon N., Chirachanchai S. 2016. Polyoxymethylene Foam: From an Investigation of Key Factors Related to Porous Morphologies and Microstructure to the Optimization of Foam Properties. *Polymer*, Volume 96(8), pp. 54–62

Marshall A.L., 2012. Examination of the Interconnectivity of SiC in a Si:SiC Composite System. *The American Ceramic Society, In: Ceramic Engineering and Science Proceedings*, Volume 33(10), No. 17, pp. 193–199

Monie F., Vidil T., Grignard B., Cramail H., Detrembleur C., 2021. Self-foaming polymers: Opportunities for the Next Generation of Personal Protective Equipment. *Materials Science and Engineering: R: Reports*, Volume 145(12). Doi: https://doi.org/10.1016/j.mser.2021.100628

Moratal D., 2010. Finite Element Analysis. *IntechOpen*, London, UK, ISBN 978-953-307-123-7

Moumen A.E., Kanit T., Imad A., Minor H.E., 2015. Computational Thermal Conductivity in Porous Materials Using Homogenization Techniques: Numerical and Statistical Approaches. *Computational Materials Science*, Volume 97, pp. 148–158

Muayad A.S., Mohammed A.D., Hamad K.M., 2020. Kinetic Study of Air Bubbles-Cetyltrimethylammonium Bromide (CTAB) Surfactant for Recovering Microalgae Biomass in a Foam Flotation Column. *International Journal of Technology*, Volume 11(3), pp. 440–449

Rainglet B., Chalamet Y., Legar´e V.B., Delage K., Forest C., Cassagnau P., 2021. Polypropylene Foams Under CO2 Batch Conditions: From Formulation and Rheological Modeling to Cell-Growth Simulation. *Polymer*, Volume 218(12)

Rende, D., Schadler, L.S. and Ozisik, R., 2013. Controlling Foam Morphology of Poly (Methyl Methacrylate) Via Surface Chemistry and Concentration of Silica Nanoparticles and Supercritical Carbon Dioxide Process Parameters. *Journal of Chemistry*, Volume 2013

Roedel S., Souza J.C.M., Silva F.S., Guimarães J.M., Fredel M.C., Henriques B., 2018. Optimized Route for The Production of Zirconia Structures With Controlled Surface Porosity for

Biomedical Application. *Ceramic International*, Volume 44(11), No. 74, pp. 22496–22503

Sharudin R.W., Ohshima M., 2012. Preparation of Microcellular Thermoplastic Elastomer Foams from Polystyrene-b-polybutadiene-b-polystyrene (SEBS) and their Blends with Polystyrene. *Journal of Applied Polymer Science*, Volume 128(4), pp. 2245–2254

Solbakken J.S., Aarra M.G., 2021. CO2 Mobility Control Improvement Using N2-Foam at High Pressure And High Temperature Conditions. *International Journal of Greenhouse Gas Control*, Volume 109(30), pp. 103392. https://doi.org/10.1016/j.ijggc.2021.103392

Sundarram S. S., Li W., 2013. On Thermal Conductivity of Micro-and Nanocellular Polymer Foams. *Journal of Applied Polymer Science*, Volume 53(9), No. 11, pp. 1901–1909

Zakyan S.E., Famili M.H.N., Ako M, 2014. Controlling Foam Morphology of PS via Surface Chemistry, Size and Concentration of Nanosilica Particles. *Journal of Material Science*, Volume 49(18), pp. 6225–6239

Zulkarnain M, Fadzil M.A., Rahida Wati Sharudin, 2017. Algorithm of Pores Distribution Model for Analysis And Measurement of Thermal Conductivity of Polypropylene Porous Material. *International Journal of Technology*, Volume 8(3), pp. 398–407